Iraqi Journal of Biotechnology, 2022, Vol. 21, No. 2, 251-267

Green Method Synthesis of Silver Nanoparticles Using Leaves Extracts of *Rosmarinus officinalis*

Ameer R. Al-Khafaji, Ahmed H. Al-Azawi [1]

Institute of Genetic Engineering and Biotechnology for Postgraduate Studies, University of Baghdad

Received: 1/6/2022 Accepted: 20/9/2022 Published: December 20, 2022

Abstract: the silver nanoparticles synthesized have to be handled by humans and must be available at cheaper rates for their effective utilization; thus, there is a need for an environmentally and economically feasible way to synthesize these nanoparticles. Therefore, this study aimed to synthesis of silver nanoparticles using phenolic compounds extracted from *Rosmarinus officinalis.* Maceration method and Soxhlet apparatus were used to prepare aqueous and methanolic *Rosmarinus officinalis* leaves extracts respectively, Furthermore, *Rosmarinus officinalis* silver nanoparticles (RAgNPs) were prepared from the aqueous and methanolic leaves extract of this plant and diagnosed using the ultraviolet (UV) spectroscopy, scanning electron microscopy (SEM), atomic fluorescence microscopy (AFM), X-ray scattering (XRD), energy dispersive X-ray (EDX) and infrared spectroscopy (FTIR). The diagnostic results showed that the nanoparticles are spherical in shape, single or combined, crystalline for both aqueous and methanolic silver nanoparticles extract.

Keywords: Rosmarinus officinalis, silver nanoparticles, FTIR, AFM, SEM, EDX, UV and XRD.

Corresponding author: (Email: ahmed@ige.uobaghdad.edu.iq)

Introduction

Nanotechnology is a field that is promising, creating an impact in all spheres of human life. Nanoparticles (NPs) are typically a cluster of atoms ranging from 1 to 100 nm in size and display new and enhanced properties based on size, distribution as well as morphology than larger particles in the bulk materials of which the nanoparticles are made (1).

The problem with most of the chemical and physical methods of nano-silver production is that they are extremely expensive and also involve the use of toxic, hazardous chemicals, which may pose potential environmental and biological risks. Biosynthesis of silver nanoparticles is a bottom-up approach that mostly involves reduction/oxidation reactions. It is majorly the microbial enzymes or the plant phytochemicals with antioxidant or reducing properties that act on the respective compounds and give the desired nanoparticles. The three major components involved in the preparation of nanoparticles using biological methods are the solvent medium for synthesis, the environmentally friendly reducing agent, and a nontoxic stabilizing agent (2). In biological methods (green synthesis), systems like bacteria (3), fungi (4) yeast (5) *cyanobacteria* (6) *actinomycetes* (7) and plants (8), have been used to synthesis of nanoparticles. Certainly, the biological synthesis of

NPs has a unique ability for the production of precise shapes and controlled structures. Also, these methods do not require any sophisticated instrumentation, simple, efficient, eco-friendly, inexpensive and safer methods (9), as well as, the plants have a broad variety of metabolites that can aid in the reduction of silver ions and are quicker than microbes during the synthesis (10).

Plants that possess different products like phenols, terpenoids, alkaloids, flavonoids, proteins, carbohydrates etc. play a key role in the stabilization and reduction of metallic silver into AgNPs, (11-12). A number of biomolecules present in the plant extract reduce the monovalent silver ion to uncharged atoms and these atoms aggregate to reach nano-size, other biomolecules of the plant extract envelope or cap them to prevent their further aggregation (13). The rich source of metabolites with negatively charged functional groups may possibly be responsible for the reduction of metal ions and efficient stabilization of synthesized NPs under natural conditions (14).

Materials and methods

Collection of *Rosmarinus officinalis L.*

Rosmarinus officinalis were obtained from the plantation in Baghdad city, identification as (*Rosmarinus officinalis L.*) by Department of Biology, College of Science, University of Baghdad. The leaves were washed with water and dried at room temperature, and ground using a grinder, then stored at 4^{o}C for further analysis.

Preparation of *Rosmarinus officinalis* extracts

Firstly, in order to defeat the leaves, 400 grams of *Rosmarinus officinalis* leaves powder was macerated with 2 litter of petroleum ether solvent. The residue was collected, air-dried and separated into two batches. Each batch of the defatted plant leaves was individually extracted with water and methanol to prepare aqueous and methanolic extracts according to N'Guessan *et al*. (15) and AACC (16) respectively.

Preparation of green silver nanoparticles using *Rosmarinus officinalis* extracts

Preparation of green silver nanoparticles by *Rosmarinus officinalis* aqueous and methanolic extracts were done according to Ojha *et al*. (17) and Krishnadhas *et al*. (18) with some modifications. Five ml of each extract was sprayed into 95 ml of 10 mM silver nitrate $AgNO_3$ solution (which was prepared by dissolving 1.69 g $AgNO_3$ into 1 L deionized water) separately dropwise with a flow rate of 0.2 ml/min under ultrasonic conditions, with an ultrasonic power of 100 W and a frequency of 42 kHz. After sonication for 20 min, the solutions were stirred at 800 rpm at 25°C for 30 min, and then kept in dark bottles at 25°C for 48 h. After 24 h the reaction mixture was purified by centrifugation for 10 min at 10000 rpm to get clear supernatant.

The final colloid samples were stored in dark bottles at 4°C. During 5 days the color of solutions was changed from dark green to light brownish green for *Rosmarinus officinalis* silver nanoparticles (RAgNPs), this change in color indicates the formation of silver nanoparticles (AgNPs).

Determination of total phenolic content

The total phenolic content of the *Rosmarinus officinalis* methanolic and the aqueous extracts were determined spectrophotometrically using the Folin-Ciocalteu method described by Jayaprakasha *et al*. (19). 0.4 ml of each sample was mixed with 2.0 ml of the Folin- Ciocalteu reagent (diluted 10 times), and 1.6 ml of 7.5% sodium carbonate solution. The total volume was adjusted to 5 ml by adding distilled water. The tubes were covered with parafilm and allowed to stand for 30 minutes at room temperature before the absorbance was read at 760 nm.

The total phenolic content was calculated from a calibration standard curve of gallic acid Figure (1) and the results were given as mg gallic acid equivalent per gram of dry weight.

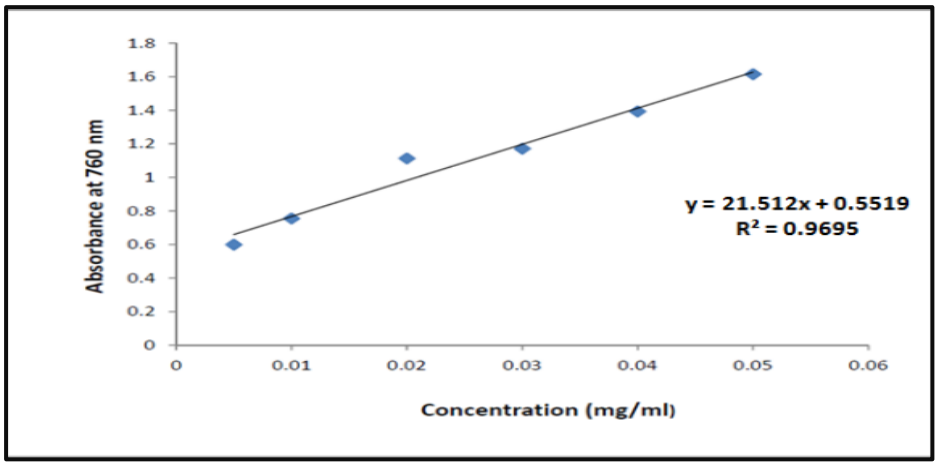

Figure (1): Standard curve of gallic acid

Characterization of the prepared nanoparticles

UV-Visible absorption spectroscopy

Absorbance spectra of AgNPs solution were measured by UV-Visible Absorption Spectroscopy (UV-VIS) double beam spectrophotometers. All spectra were measured at room temperature in a quartz cell with a 1 cm optical path. Deionized distilled water was used as a blank. The absorption was taken from (200-800nm). Some concentrated samples were diluted 1: 10 in deionized water (20).

Scanning electron microscopy analysis

A scanning electron microscope (SEM) was employed to analyze the morphology of the nanoparticles that were formed. The morphological characterization of the samples was done using mira3 Tescan for SEM analysis. The samples were prepared according to the standard procedures, by dispersing them on a glass slide (Almost Seven drops on the slide). After that, the sample was subjected to examination, and then readings were taken at a magnification of 5000x, 10000x, 20000x, 50000x with steady voltage (21).

Atomic force microscopy

Atomic force microscopy (AFM) is one of the first tools for imaging, measuring, and manipulating materials at the nanoscale. It provides 3D imaging capability and qualitative and quantitative information for many physical properties including size,

morphology, surface texture, and roughness (22). A thin film of the sample from each type of nanoparticles was placed on a glass slide by dropping 100 µl of the sample on the slide and was allowed to dry for 5 min. The slides were then scanned with the AFM (23).

X-ray diffractometer

The analysis using an X-ray diffractometer (XRD) is useful for knowing the phase structure and purity of synthesized green AgNPs and is generally used as a common technique to study the phase composition and crystal structure of AgNPs. A thin film of uniform water suspended from each type of nanoparticle was prepared on a glass slide and kept for drying. X-ray diffraction (XRD) pattern was recorded by employing an X-ray diffractometer at 2θ/θ scanning mode (operational voltage 40 kV and current 30 mA, Cu K (a) radiation λ = 1.540) (17). Data were recorded for the 2θ range of 10 to 80 degrees with a step of 0.0200 degrees. The result obtained from the XRD pattern was interpreted with standard reference of the Joint Committee on Powder Diffraction Standards (JCPDS card number 04-0783) for the characterization of AgNPs (24). The particle size of the prepared samples was determined by using Debye–Scherrer equation as follows:

$$D=0.9\lambda/\beta \cos\theta$$

Where D is the crystal size, λ is the wavelength of x-ray, θ is the diffraction angle (Braggs angle) in radians and β is the full width at half maximum of the peak in radians (25).

Energy dispersive X-ray

Energy-dispersive X-ray (EDX) analysis was carried out using a JEOL JEM 2100 high-resolution transmission electron microscope to confirm the presence of silver in the minutes and to detect other elemental structures of the particles (26).

Fourier transform infrared (FTIR) Spectroscopy analysis

The characterization of functional groups on the surface of AgNPs by plant extracts was investigated by FTIR analysis (Shimadzu) and the spectra were scanned in the range of 4000–400 cm^{-1} range at a resolution of 4 cm^{-1}. The samples were prepared according to the standard procedures, by dispersing them on a glass slide. After that, the sample was subjected to examination (27).

Results and discussion

Total phenolic content of *Rosemary officinalis* leaves extracts

Numerous phenolic compounds have been studied for their biological properties and benefits to human health (28-29). The total phenolic contents of the aqueous and methanolic extracts were evaluated by using Folin-Ciocalteu reagent. The results showed that the total phenolic content (TPC) of the *Rosemary officinalis* extracts increased gradually with increases in the concentration, with significant differences ($P \leq 0.01$). The highest values were 10.15 ±0.03 and 14.24 ±0.01 mg/g in 50 mg/ml in both methanolic and aqueous extracts, respectively, as shown in Table (1). This result revealed that TPC in *Rosemary officinalis* aqueous extract was more than TPC in methanolic extracts. A recent investigation including several rosemary species revealed amounts of total phenolics in plant leaves (30-31).

Table (1): Total phenolic content of *Rosmarinus officinalis* extracts

Concentration (mg\ml)	Methanolic extract (mg\g)	Aqueous extract (mg\g)	LSD value
12.5	3.87 ±0.01	4.78 ±0.01	0.048**
25	6.08 ±0.12	8.20 ±0.02	0.335**
50	10.15 ±0.03	14.24 ±0.01	0.098**
LSD value	0.225**	0.053**	-------

Biosynthesis and characterization of nanoparticles

In this study, the formation of silver nanoparticles was monitored depending on color change and UV spectroscopy absorption. The colors of the green silver nanoparticle solutions were changed from dark green to light brownish green for *Rosemary officinalis* silver nanoparticles (RAgNPs), with the addition of *Rosemary officinalis* methanolic and aqueous extracts, respectively, to silver nitrate solution. The color began to change after 24 hours, and for 48 hour the color changed to the final color (Figure 2). This change in color indicates the formation of silver nanoparticles (AgNPs) due to the reduction of silver metal ions Ag^{+} into silver nanoparticles Ag^{0} via the active molecules present in the *Rosemary officinalis* methanolic and aqueous extracts. The silver nanoparticles were prepared using *Rosemary officinalis* methanolic and aqueous extracts. The biosynthesis of metallic nanoparticle using plant extracts in comparison with other bioreductants is more fruitful in terms of its ease (32). It is well known that the phytochemicals not only reduce the Ag^{+} into Ag^{0} but also are responsible for its capping to make these nanoparticles highly stable (33-35). Plants possess different metabolites like phenols, terpenoids, alkaloids, flavonoids, proteins, carbohydrates etc. play a key role in stabilization and reduction of metallic silver into AgNPs (11, 17). The reduction rate and formation of nanoparticles can be increased further by increase the incubation time so the intensity of the color increased with increasing the time of reaction (36). Metal nanoparticles show different colors in solution due to their optical properties (37). The change in color is referred to excitation of surface plasmon Resonance (SPR) in metal nanoparticles. Silver nanoparticles exhibit interesting optical properties directly associated with localized surface plasmon resonance which is highly depends on the morphology of the nanoparticles (38). This result is agreed with Saliem *et al*. (36) and Thamer (39) they reported that reduction of silver ion into silver nanoparticles during exposure to the plant extracts could be followed by color change. Therefore, the characterization of AgNPs is important for evaluating the functional aspects of the synthesized particles.

Figure (2): Color change of RAgNPs methanolic and aqueous extract after 48 hours

UV-Visible spectroscopy

UV–visible spectroscopy is a primary step in confirmation of the synthesis of Ag-NPs as well as the color change. When the *Rosemary Officinalis* extract was mixed with an aqueous solution of $AgNO_3$, this resulted in a change of color. This change in color is a result of the collective oscillation of free electron of silver nanoparticles in resonance with the light wave in silver nanoparticle synthesis and this oscillation gives a typical peak value. Figures (3, 4 and 5) showed UV- visible spectra of the plant extracts alone and with AgNO3 solution. The weak absorption peak at 200 nm indicates the presence of several organic compounds which are known to interact with silver ions (40-41). The surface plasmon resonance absorbance is exceptionally sensitive to the nature, size, and shapes of the NPs formed dielectric constant of the medium and temperature, and their inter particle distances (42). The absorption spectrum was recorded between 200 nm and 800 nm. It is observed that the silver surface plasmon resonance band centered at 234 nm in the (RAgNPs) methanolic extract and 216 nm in the aqueous (RAgNPs) extract, in comparison with UV Test for *Rosemary officinalis* methanolic and aqueous extract (224 and 279) nm respectively, in addition to the UV test for silver solution (216) nm.

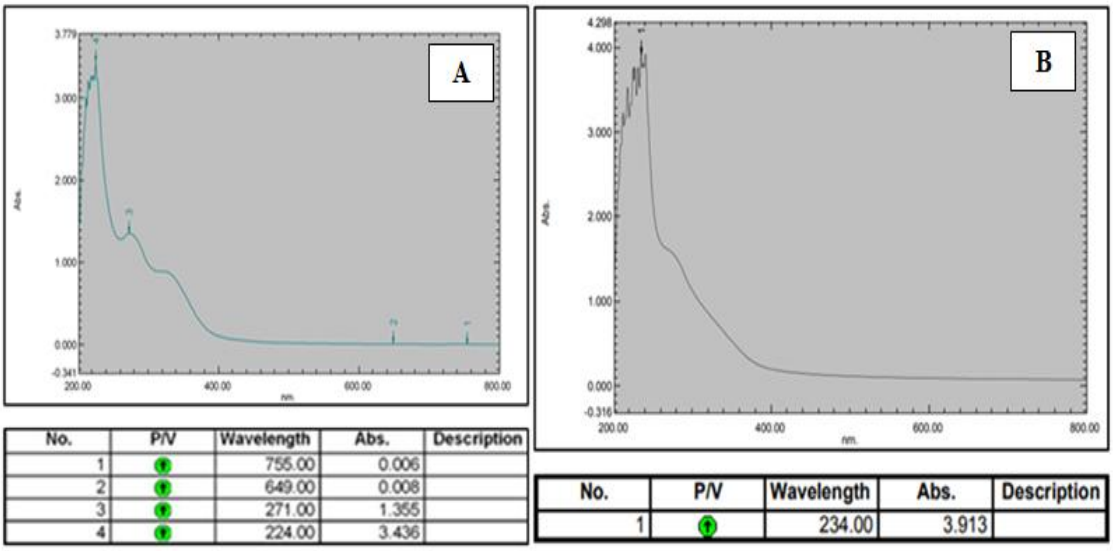

No.	P/V	Wavelength	Abs.	Description
1	↑	755.00	0.006	
2	↑	649.00	0.008	
3	↑	271.00	1.355	
4	↑	224.00	3.436	

No.	P/V	Wavelength	Abs.	Description
1	↑	234.00	3.913	

Figure (3): UV-Visible spectral analysis of (A): *R. officinalis* methanolic extract, (B): synthesized (RAgNPs) methanolic extract

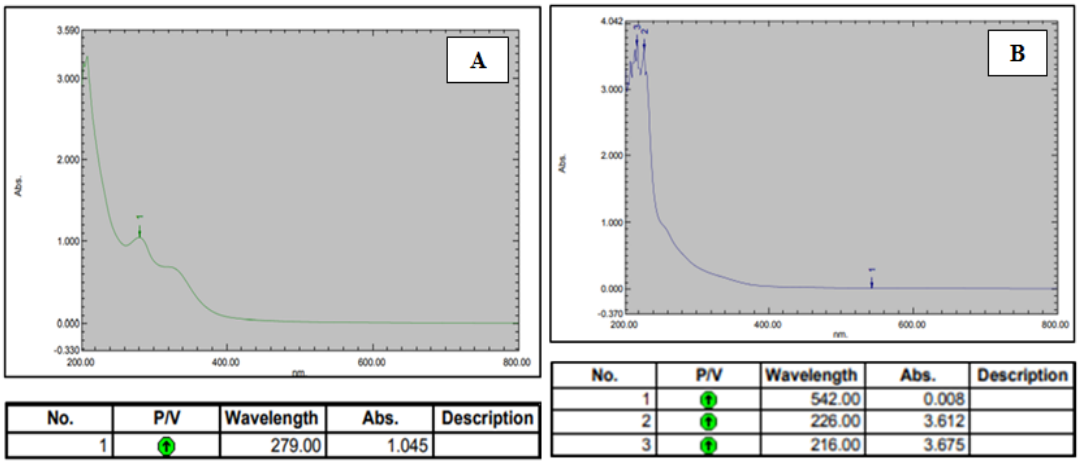

No.	P/V	Wavelength	Abs.	Description
1	↑	279.00	1.045	

No.	P/V	Wavelength	Abs.	Description
1	↑	542.00	0.008	
2	↑	226.00	3.612	
3	↑	216.00	3.675	

Figure (4): UV-Visible spectral analysis of (A): *R. officinalis* aqueous extract, (B): synthesized (RAgNPs) aqueous extract

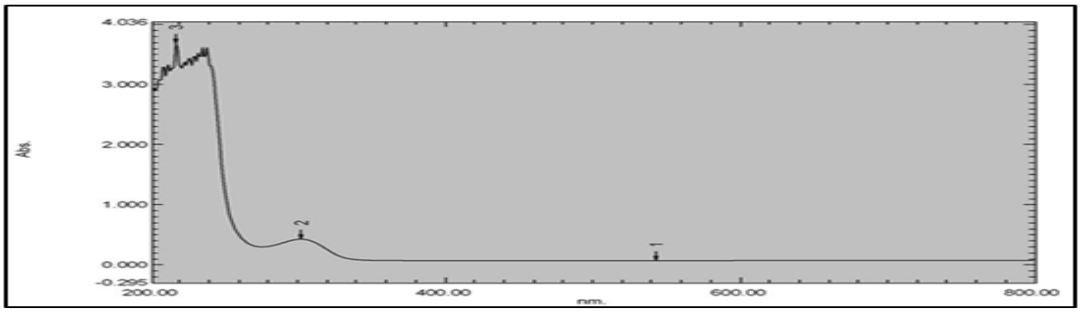

No.	P/V	Wavelength	Abs.	Description
1	↑	542.00	0.068	
2	↑	301.00	0.424	
3	↑	216.00	3.675	

Figure (5): UV-Visible spectral analysis of (AgNO3)

Scanning electron microscope

Scanning Electron Microscopy (SEM) is one of the widely used techniques for the characterization of the synthesized nanoparticles, and the shape and morphology of the green nanoparticles formed were analyzed by this microscopy. The observations confirm that the morphology of nanoparticles is highly variable with a variety of sizes and shapes. The surface of Ag-NPs has been studied using a scanning electron microscope (SEM). The results of SEM analysis showed the particles are spherical in shape (this is for 2 types of synthesized nanoparticles), with nanometer in size for RAgNPs of the methanolic and aqueous extract (Figures 6 and 7). Large nanoparticles were seen due to aggregation. This aggregation took place due to the presence of cell components on the surface of nanoparticles and acts as a capping agent (43). This result was in agreement with Surega, (44) who observed the morphology of the synthesized AgNPs using aqueous leaf extracts of *Tridax procumbens*, *Euphorbia hirtaand* and *Azardirachta indica* through SEM. The observations revealed that the AgNPs were spherical in their shape and agglomerated. In a previous study for the synthesis of silver nanoparticles from *Crocus sativus* L extract, SEM analysis showed the average particle size of 20–30 nm as well as it is spherical in shape (39). SEM figure of the AgNPs synthesized by extract of *Phyllanthus niruri* under optimized physical conditions revealed that the AgNPs are around 100 nm in size with the mixture of many shapes i.e. triangle, rhombus, and spherical are clearly observed and spherical are predominant. SEM determination showed the formation of AgNPs, which were well dispersed and the aggregation of the particles could be seen (45).

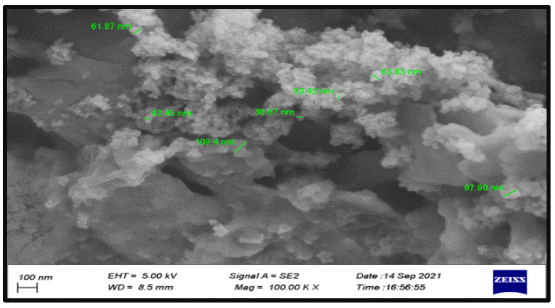

Figure (6) SEM image showed the shape and size of RAgNPs methanolic extract

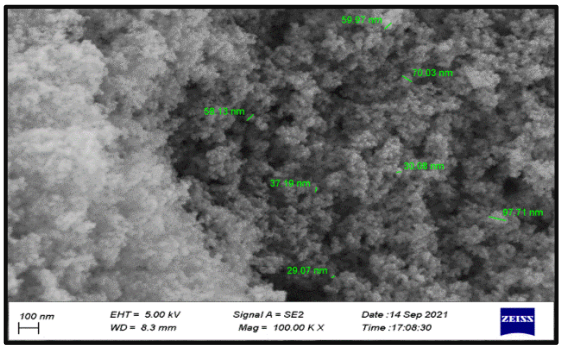

Figure (7) SEM image showed the shape and size of RAgNPs aqueous extract

Atomic force microscopy (AFM)

The results of AFM analysis showed both the two-dimensional and three-dimensional views of RAgNPs methanolic and aqueous extract were spherical in shape, single or in aggregates, AFM analysis also showed that the average size of particles was 18.66 and 44.49 nm for RAgNPs aqueous and methanolic extract respectively (Figures 8 and 9). This finding was in agreement with Korbekandi *et al*. (46), they showed that the biosynthesized silver nanoparticles were almost spherical, single (25-50 nm), or in aggregates (100 nm).

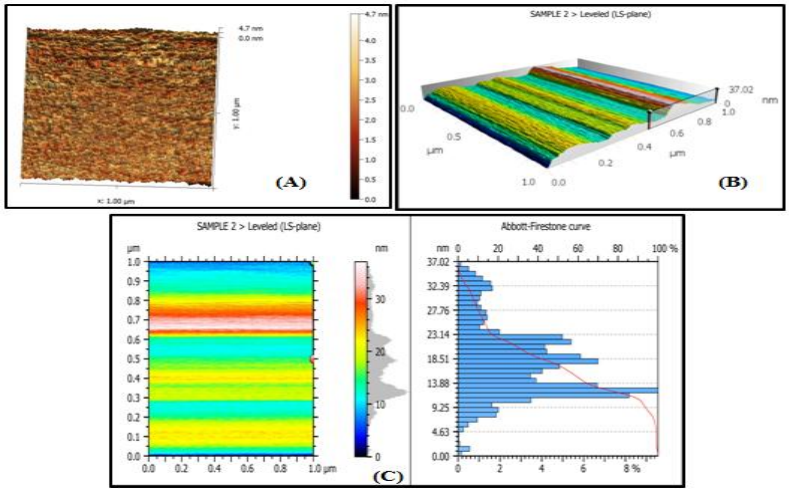

Figure (8): Atomic force microscopy analysis of RAgNPs aqueous extract (A): Two-dimensional of RAgNPs aqueous extract, (B): Three-dimensional of RAgNPs aqueous extract, (C): AFM diagram of size range of RAgNPs aqueous extract.

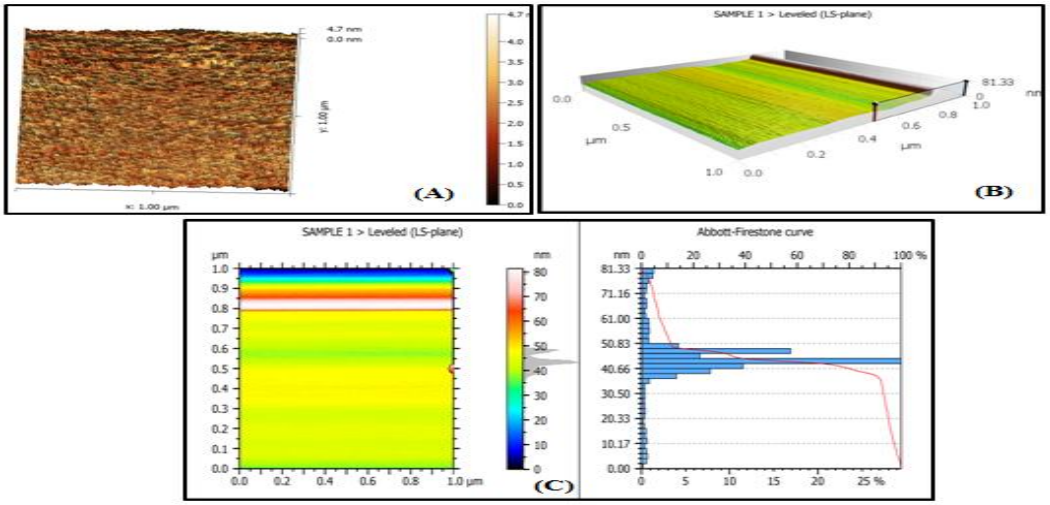

Figure (9): Atomic force microscopy analysis of RAgNPs methanolic extract (A): Two-dimensional of RAgNPs methanolic extract, (B): Three-dimensional of RAgNPs methanolic extract, (C): AFM diagram of size range of RAgNPs methanolic extract

X-ray diffractometer

X-ray diffractometer (XRD) is powerful technique for characterizing crystalline materials provides information on structures, phases, preferred crystal orientations, and other structural parameters, such as average

grain size, crystallinity, strain, and crystal defects (47).

The green synthesis of AgNPs was further supported by X-ray diffraction (XRD). Figure (10) recorded obvious diffraction peaks at 2θ values 38.868, 44.116, 64.278, 77.250 for RAgNPs methanolic extract which were corresponded to 111, 200, 220 and 311 planes of silver, and figure (11) showed diffraction peaks at 2θ values 37.922, 47.842, 64.255, 77.215 of RAgNPs aqueous extract corresponded to 111, 200, 220 and 311 planes of silver.

XRD pattern clearly showed that the AgNPs formed by the reduction of Ag^{+} ions using *Rosemary officinalis* extracts are crystalline in nature. Some unassigned peaks were observed, it may be due to the bio-organic phase/ metalloproteins occurring on the surface of silver nanoparticles (11, 48) or it may be due to the fewer biomolecules of stabilizing agents such as enzymes or proteins in the plant extract (49-50).

The average nanocrystalline size has been estimated by using well known Debye–Scherrer formula, $D = k\lambda/\beta\cos\theta$, where D is particle diameter size, k is a constant equal 1, λ is wavelength of x-ray source (1.540 A°), β is the full width at half maximum (FWHM) = 0.23, θ is the diffraction angle for strongest three peaks. The average crystallites sizes according to Debye– Scherrer equation calculated are found to be 23.37 nm and 31.43 nm for RAgNPs aqueous and methanolic extract respectively. This finding is agree with the study by Sathishkumar *et al*. (51) was involved synthesis of silver nanoparticle using aqueous extract of *Cinnamon zylanicum* bark, silver nanoparticles have shown clear peaks of cubic phases at 38.2 (111), 44.5 (200), 64.5 (220) and 77.6 (311). Many reports describe that the NPs synthesized by reacting $AgNO_3$ with biological solutions are face centered cubic with minor variations in peak values depending upon nature of extract; metabolites present and binding properties (52). Interestingly, most of researchers (53-55, 47) that synthesized the nanoparticles using plant extracts seem to obtained a similar crystal structure.

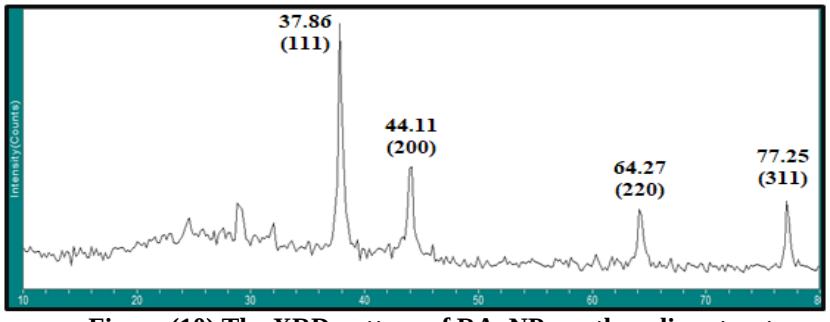

Figure (10) The XRD pattern of RAgNPs methanolic extract

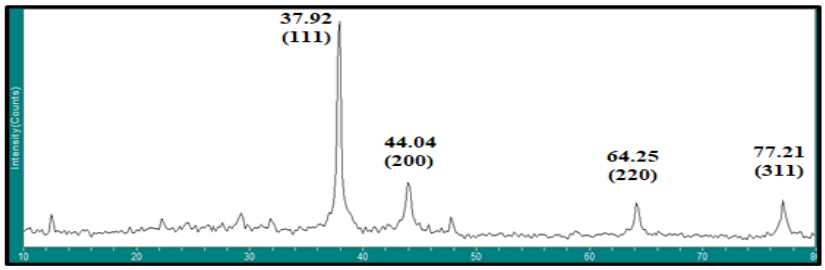

Figure (11) The XRD pattern of RAgNPs aqueous extract

Energy Dispersive X-ray (EDX)

Energy-dispersive X-ray (EDX) spectroscopy confirmed the presence of silver within the nanoparticles of the methanolic and aqueous extract of rosemary leaves; the EDX spectrum recorded a peak for silver at the level of 3 kV, which confirms the presence of silver in nanoparticles (Figures 12 and 13). These results agree with Jegadeeswaran *et al*. (56) as it was found that the nano-solution of *Padina tetrastromatica* extract recorded a sharp peak between 2.7 - 4 kV EDX spectrum, which confirms the presence of silver. EDX analysis detected the presence of elements within the selected area and found that the Ag was the major element with oxygen (O_2), nitrogen (N) and sodium (Na), silicon (Si) in the sample

.

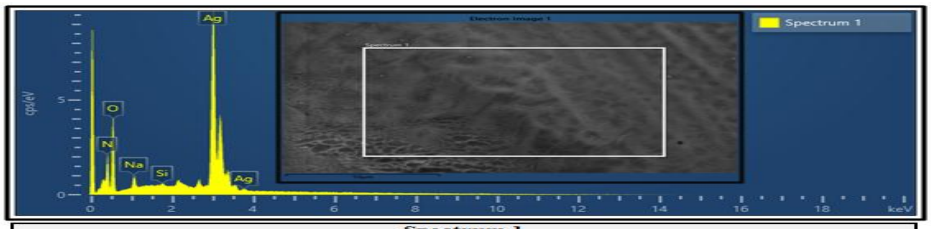

Spectrum 1				
Element	Line Type	Weight %	Weight % Sigma	Atomic %
N	K series	21.30	0.55	38.42
O	K series	31.22	0.41	49.32
Ag	K series	46.15	0.43	10.81
Na	K series	1.22	0.06	1.34
Si	K series	0.12	0.03	0.10
Total		100.00		100.00

Figure (12): The silver recording is shown at the kV energy level in the methanolic (RAgNPs) extract

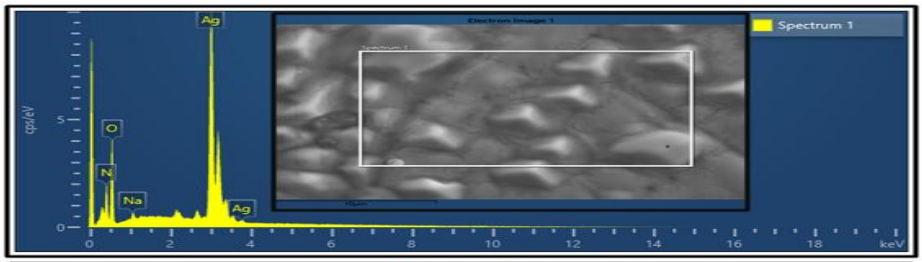

Spectrum 1				
Element	Line Type	Weight %	Weight % Sigma	Atomic %
O	K series	31.01	0.41	49.64
Ag	K series	47.39	0.43	11.25
N	K series	21.05	0.55	38.49
Na	K series	0.56	0.06	0.62
Total		100.00		100.00

Figure (13): The silver recording is shown at the kV energy level in the aqueous (RAgNPs) extract

Fourier transformation infrared spectroscopy (FTIR)

Fourier transformation infrared spectroscopy (FTIR) analysis was employed to identify functional groups that may be responsible for the reduction/ bio-reduction of $AgNO_3$ to Ag-NPs and their stabilization. FTIR spectroscopy is a technique used to measure the vibration frequencies of the bonds in molecules. It is used to confirm the presence of the functional groups of the active components in the synthesized AgNPs based on the band value in the region of the infrared radiation (57). The dual role of the plant extract as a bioreduction and capping agent was confirmed by FTIR analysis of the prepared AgNPs of *Rosemary officinalis* leaves extract.

Fourier Transform Infra-Red (FTIR) spectrophotometers were used for recording spectra in the region 4000 cm–1 to 670 cm–1 (2.5μm to 15 μm) or

in some cases down to 200 cm–1 (50 μm). The results of the FTIR Spectra of the *Rosemary officinalis* methanolic and aqueous extracts revealed the presence of different functional groups such as Phenolic– OH group stretching, C-H stretching, N-H bend, C-C stretching and C-N stretching, and had prominent bands of absorbance at peaks (3367.71, 2929.87, 1612.49, 1413.82, and 1072.42) cm^{-1} for methanolic extract and (3365.78, 2929.87, 1606.7, 1413.82, and 1080.14) cm^{-1} for aqueous extract respectively (Table 2). In addition, the FTIR Spectra of the $AgNO_3$ which had prominent band of absorbance at peaks (1379.1) cm^{-1}. Moreover, the FTIR spectroscopy showed that samples analysis had prominent bands of absorbance at peaks (1076.28, 1382.96, 1620.21 and 3169.04) cm^{-1} for methanolic (RAgNPs) extract, and the absorption bands appeared at (1101.35, 1382.96, 1627.92, 2926.01, and 3402.43) cm^{-1} for the aqueous (RAgNPs) extract (Figures 14 and 15).

The peak (1382.96) in the FTIR Spectra of the methanolic and aqueous (RAgNPs) extract, is the same peak found in the AgNO3 sample and it was not found in the *Rosemary officinalis* methanolic and aqueous extract, therefore, this indicates the formation of (AgNPs). Das *et al*. (58) and (59) mention the changes in the functional groups in active biomolecules might suggest their involvement in the synthesized of (AgNPs).

Table (2): IR frequencies region for the functional groups of the *R. officinalis* leaves extracts

The Functional Group	I.R. wave number Standard groups	I.R. wave number of methanolic extract	I.R. wave number of aqueous extract	I.R. wave number of methanolic (RAgNPs) extract	I.R. wave number of aqueous (RAgNPs) extract
Phenolic–OH group stretching	3650-2500	3367.71	3365.78	3169.04	3402.43
C-H stretching	2960-2850	2929.87	2929.87	-----	2926.01
N-H bend	1650-1580	1612.49	1606.70	1620.21	1627.92
C-C stretching	1500-1400	1413.82	1413.82	-----	------
C-N stretching	1250-1020	1072.42	1080.14	1076.28	1101.85

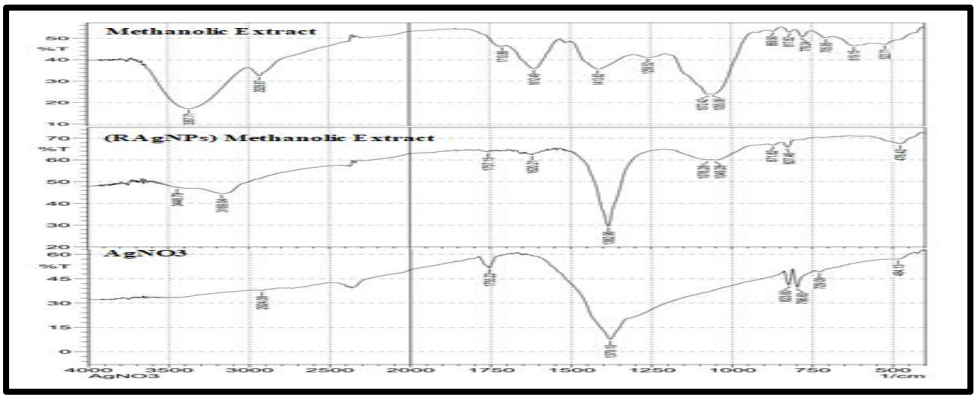

Figure (14): FTIR Spectra Pattern of *Rosemary officinalis* methanolic extract, (RAgNPs) methanolic extract and $AgNO_3$

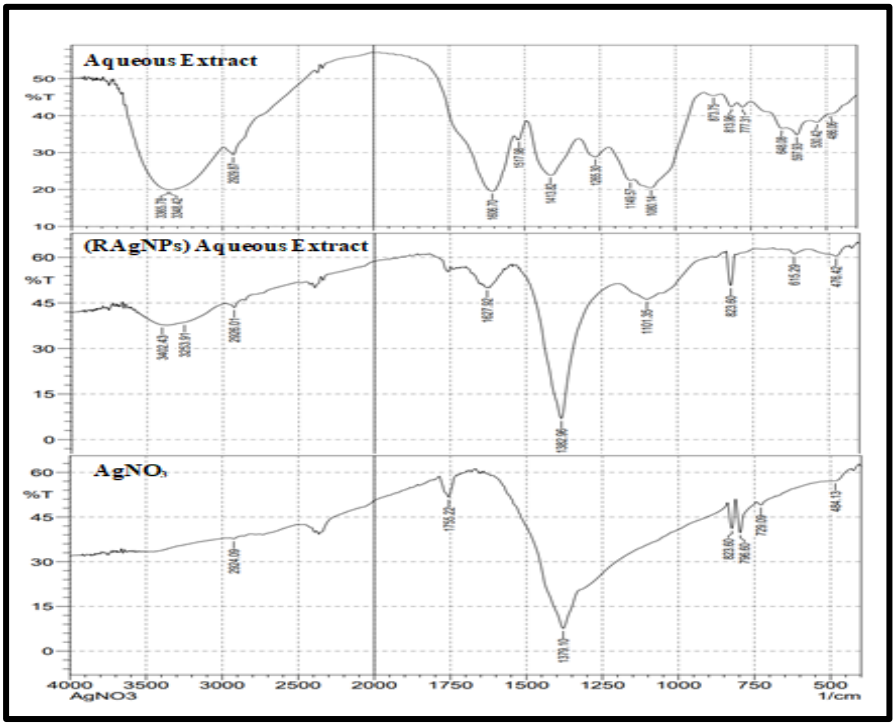

Figure (15): FTIR Spectra Pattern of *Rosemary officinalis* aqueous extract, (RAgNPs) aqueous extract and $AgNO_3$

Conclusion

This study concluded that the total phenolic contained in *Rosemary officinalis* aqueous extract was more than methanolic extracts, as well as, the extracts of *Rosmarinus officinalis* leaves can be utilized as a good reductant for the non-toxic or green synthesis of metal silver nanoparticles.

References

1. Bae, E.; Park, H. J.; Lee, J.; Kim, Y.; Yoon, J.; Park, K.; Choi, K. and Yi, J. (2010). Bacterial cytotoxicity of the silver nanoparticle related to physicochemical metrics and agglomeration properties. Environmental Toxicology and Chemistry, 29(10): 2154-2160.
2. Prabhu, S. and Poulose, E. K. (2012). Silver nanoparticles: mechanism of antimicrobial action, synthesis, medical applications, and toxicity effects. International Nano Letters, 2:32.
3. Kumar, C. G. and Mamidyala, S. K. (2011). Extracellular synthesis of silver nanoparticles using culture supernatant of *Pseudomonas aeruginosa. Coll. Surf. B:* Biointerfaces, 84: 462-466.
4. Rodriques, A. G.; Ping, L. Y.; Marcato, P. D.; Alves, O. L.; Silva, M. C. P.; Ruiz, R. C.; Melo, I. S.; Tasic, L. and DeSouza, A. O. (2012). Biogenic antimicrobial silver nanoparticles produced by fungi. Applied Microbiology Biotechnology, 97(2): 775-782.
5. Seshadri, S.; Saranya, K. and Kowshik, M. (2011). Green synthesis of lead sulfide nanoparticles by the lead resistant marine yeast, Rhodosporidium diobovatum. Biotechnol. Prog., 27: 1464-1469.
6. Lengke, M.; Fleet, M. E. and Southam, G. (2006). Morphology of gold nanoparticles synthesized by filamentous cyanobacteria from gold (I)–thiosulfate and gold (III)–chloride complexes. Langmuir, 22: 2780-2787.
7. Sastry, M.; Ahmad, A.; Islam Khan, M. and Kumar, R. (2003). Biosynthesis of metal nanoparticles using fungi and

actinomycetes. Current Science., 85: 162-170.

8. Shankar, S. S.; Rai, A.; Ankamwar, B.; Singh, A.; Ahmad, A. and Sastry, M. (2004). Rapid synthesis of Au, Ag, and bimetallic Au core–Ag shell nanoparticles using Neem (*Azadirachta indica*) leaf broth.
9. Gurunathan, S.; Kalishwaralal, K.; Vaidyanathan, R.; Venkataraman, D.; Pandian, S. R. K.; Muniyandi, J.; Hariharan, N. and Eom, S. H. (2009). Biosynthesis, purification and characterization of silver nanoparticles using *Escherichia coli*. Colloids and Surfaces B: *Biointerfaces*, 74(1): 328-335.
10. Jha, A. K.; Prasad, K. and Prasad, D. (2009). A green low-cost biosynthesis of Sb20 nanoparticles. Biochemical. England. Journal, 43: 303-306.
11. Vanaja, M. and Annadurai, G. (2013). *Coleus aromaticus* leaf extract mediated synthesis of silver nanoparticles and its bactericidal activity. Applied Nanoscience, 3(3): 217-223.
12. AL-Azawi, A. H. and Hassan Z. H. (2017). Antibacterial Activity of *Arachis hypogaea* L. Seed Coat Extract Cultivated in Iraq. Pakistan Journal Biotechnology., 14 (4): 601-605.
13. Ganaie, S. U.; Abbasi, T.; Anuradha, J. and Abbasi, S. A. (2014). Biomimetic synthesis of silver nanoparticles using the amphibious weed ipomoea and their application in pollution control. Journal of King Saud University-Science, 26(3): 222-229.
14. Banerjee, P. and Nath, D. (2015). A phytochemical approach to synthesize silver nanoparticles for non-toxic biomedical application and study on their antibacterial efficacy. Nanoscience Technology., 2: 1-14.
15. N'Guessan, J. D.; Bidie, A. P.; Lenta, B. N.; Weniger, B.; Andre, P. and Guina, F. (2007). In vitro assays for bioactivity-guided isolation of anti-salmonella and antioxidant compounds in Thon ninja sanguine flowers. African Journal of Biotechnology, 6:1685-1689.
16. American Association of Cereal Chemists (AACC) (1984). Method 08-01. The Association St. Paul, M. N.
17. Ojha, S.; Sett, A. and Bora, U. (2017). Green synthesis of silver nanoparticles by *Ricinus communis* var. carmencita leaf extract and its antibacterial study. Advances in Natural Sciences: Nanoscience and Nanotechnology, 8(3): 35-39.
18. Krishnadhas, L.; Santhi, R. and Annapurani, S. (2017). Green Synthesis of Silver Nanoparticles from the Leaf Extract of *Volkameria inermis*. *International* Journal of Pharmaceutical and Clinical Research, 9(8): 610-616.
19. Jayaprakasha, G. K.; Singh, R. P. and Sakariah, K. K. (2001). Antioxidant activity of grape seeds (*Vitis vinifera*). Food Chemistry, 73: 285- 290.
20. Carrillo-Lopez, L. M.; Zavaleta-Mancera, H. A.; Vilchis-Nestor, A.; Soto-Hernandez, R. M.; Arenas-Alatorre, J.; Trejo-Téllez, L. I. *et al*. (2014). Biosynthesis of silver nanoparticles using *Chenopodium ambrosioides*. Journal of Nanomaterials
21. Dimitrijevic, R.; Cvetkovic, O.; Miodragović, Z; Simic, M; Manojlović, D. and Jovic, V. (2013). SEM/EDX and XRD characterization of silver nanocrystalline thin film prepared from organometallic solution precursor. Journal Mineral Metall. Sect. B-Metall., 49(1): 91-95.
22. Chaudhuri, S. K.; Chandela, S. and Malodia1, L. (2016). Plant Mediated Green Synthesis of Silver Nanoparticles Using *Tecomella undulata* Leaf Extract and Their Characterization. Nano Biomed Engineering., 8(1): 1-8.
23. Hemath Naveen, K. S.; Kumar, G.; Karthik, L. and Bhaskara Rao, K. V. (2010). Extracellular biosynthesis of silver nanoparticles using the filamentous fungus *Penicillium* sp. Archives Applied Science Research, 2(6): 161-167.
24. Anandalakshmi, K.; Venugobal, J. and Ramasamy, V. (2016). Characterization of silver nanoparticles by green synthesis method using *Pedalium murex* leaf extract

and their antibacterial activity. Applied Nanoscience , 6: 399-408.

25. Sarvamangala, D.; Kondala, K.; Murthy, U. S. N.; Rao, B. N.; Sharma, G. V. R. and Satyanarayana, R. (2013). Biogenic Synthesis of AG 's Using *Pomelo* Fruit – Characterization and Antimicrobial Activity against Gram+ve and Gram-ve Bacteria. International Journal Pharmaceutical Science Review Research., 19(2): 30-35.
26. Baygar, T.; Sarac, N.; Ugur, A. and Karaca, I. R. (2019). Antimicrobial characteristics and biocompatibility of the surgical sutures coated with biosynthesized silver nanoparticles. Bioorganic chemistry, 86: 254-258.
27. Iravani, S.; Korbekandi, H.; Mirmohammadi, S. V. and Zolfaghari, B. (2014). Synthesis of silver nanoparticles: chemical, physical and biological methods. Research in pharmaceutical sciences. 9(6): 385.
28. Kallscheuer, N.; Vogt, M. and Marienhagen, J. A. (2017). Novel Synthetic Pathway Enables Microbial Production of Polyphenols Independent from the Endogenous Aromatic Amino Acid Metabolism. American Chemistry Society Synthesis Biology, 6:410-415.
29. AL-Azawi, A. H. (2017). Phytochemical, Antibacterial and antioxidant activities of *dodonea viscosa Jacq*. extracts cultivated in Iraq. Iraqi Journal of Biotechnology 16(4): 37-46.
30. Yeddes, W.; Chalghoum, A.; Aidi-Wannes, W.; Ksouri, R. and Saidani Tounsi, M. (2019). Effect of bioclimatic area and season on phenolics and antioxidant activities of rosemary (*Rosmarinus officinalis* L.) leaves. Journal of Essential Oil Research, *31*(5), 432-443.
31. Kheiria, H.; Mounir, A.; María, Q.; José, J. M. and Bouzid, S. (2021). Total Phenolic Content and Polyphenolic Profile of Tunisian Rosemary (*Rosmarinus officinalis* L.) Residues. In *Natural Drugs from Plants*. IntechOpen.
32. Bhadra, M. P.; Sreedhar, B. and Patra, C. R. (2014). Potential theranostics application of bio-synthesized silver nanoparticles (4-in-1 system). Theranostics ,4:316–335.
33. Arokiyaraj, S.; Vincent, S.; Saravanan, M.; Lee, Y.; Oh, Y. K. and Kim, K. H. (2017). Green synthesis of silver nanoparticles using *Rheum palmatum* root extract and their antibacterial activity against *Staphylococcus aureus* and *Pseudomonas aeruginosa*. *Artif.* Cells Nanomed Biotechnology., 45:372–379.
34. Obiazikwor, O. H. and Shittu, H. O. (2018). Antifungal activity of silver nanoparticles synthesized using Citrus sinensis peel extract against fungal phytopathogens isolated from diseased tomato (*Solanum lycopersicum* L.). Biological Sciences and Pharmaceutical Research, 6(3): 30-38.
35. Salleh, A.; Naomi, R.; Utami, N. D.; Mohammad, A-W.; Mahmoudi, E.; Mustafa, N. *et al*. (2020). The potential of silver nanoparticles for antiviral and antibacterial applications: A mechanism of action. Nanomaterials, 10:1566, 20pages.
36. Saliem, A. H.; Ibrahim, O. M. and Salih, S. I. (2016). Biosynthesis of Silver Nanoparticles using *Cinnamon zeylanicum* Plants Bark Extract. Kufa Journal For Veterinary Medical Sciences, 7(1): 51- 63.
37. Vanaja, M.; Rajeshkumar, S.; Paulkumar, K.; Gnanajobitha, G.; Malarkod, C. and Annadurai, G. (2013). Kinetic study on green synthesis of silver nanoparticles using *Coleus aromaticus* leaf extract. Advances in Applied A Science Research, 4(93): 50-55.
38. Kouvaris, P.; Delimitis, A.; Zaspalis, V.; Papadopoulos, D.; Tsipas, S. A. and Michailidis, N. (2012). Green synthesis and characterization of silver nanoparticles produced using *Arbutus Unedo* leaf extract. Materials Lett, 76: 18-20.
39. Thamer, N. A. (2016). Green Synthesis of Silver Nanoparticles Using *Crocus Sativus* L. Extracts and Evaluation of some Biological Effects in Induced Pre-Hepatocellular Carcinoma in Male Rats. PhD Thesis, College of Science, University of Babylon, Iraq.

40. Ahmad, N.; Sharma, S.; Singh, V. N.; Shamsi, S. F.; Fatma, A. and Mehta, B. R. (2011). Biosynthesis of silver nanoparticles from *Desmodium triflorum*: a novel approach towards weed utilization. Biotechnol. Research International 2011: 1-8.
41. Femi-Adepoju, A. G.; Dada, A. O.; Otun, K. O.; Adepoju, A. O. and Fatoba, O. P. (2019). Green synthesis of silver nanoparticles using terrestrial fern (*GleicheniaPectinata* (Willd.) C. Presl.): characterization and antimicrobial studies. Heliyon, 5(4): e01543.
42. Mahmoud, M. A.; Chamanzar, M.; Adibi, A. and El-Sayed, M. A. (2012). Effect of the dielectric constant of the surrounding medium and the substrate on the surface plasmon resonance spectrum and sensitivity factors of highly symmetric systems: silver nanocubes. Journal of the American Chemical Society. 134(14): 6434-6442.
43. Pirtarighat, S.; Maryam, G. and Saeid, B. (2018). Green synthesis of silver nanoparticles using the plant extract of *Salvia spinosa* grown in vitro and their antibacterial activity assessment. Journal of Nanostructure in Chemistry 018-0291-4.
44. Surega, R. (2015). Green synthesis of bioactive silver nanoparticles using plant extracts and their antinemic properties. PhD. Thesis, College of Agricalture, Tamil Nadu Agricultural University, Coimbatore.
45. Rajoriya, I. P. (2017). Green synthesis of silver nanoparticles, their characterization and antimicrobial potential. PhD thesis, Jacob Institute of Biotechnology & Bioengineering, Sam Higginbottom University of Agriculture, Technology & Sciences, Allahabad, India.
46. Korbekandi, H.; Iravani, S. and Abbasi, S. (2012). Optimization of biological synthesis of silver nanoparticles using *Lactobacillus casei* subsp. casei. Journal of Chemical Technology & Biotechnology, 87(7): 932-937.
47. Salari, S.; Bahabadi, S. E.; Samzadeh-Kermani, A. and Yosefzaei, F. (2019). In-vitro evaluation of antioxidant and antibacterial potential of green synthesized silver nanoparticles using Prosopisfarcta fruit extract. Iranian Journal of Pharmaceutical Research, 18 (1): 430-445.
48. Saware, K.; Sawle, B.; Salimath, B.; Jayanthi, K. and Abbaraju, V. (2014). Biosynthesis and characterization of silver nanoparticles using *Ficus benghalensis* leaf extract. International Journal of Research in Engineering and Technology, 3(5): 867-874.
49. Gondwal, M. and Pant, G. J. N. (2013). Biological evaluation and green synthesis of silver nanoparticles using aqueous extract of *calotropis procera* . International Journal Pharmaceutical Biological Sciences, 4 (4): 635-643.
50. Anuj, S. A. and Ishnava, K. B. (2013). Plant mediated synthesis of silver nanoparticles by using dried stem powder of *Tinospora cordifolia*, its antibacterial activityand comparison with antibiotics. Int J Pharm Bio Sci. Oct., 4(4): 849-863.
51. Sathishkumar, M.; Sneha, K.; Won, S. W.; Cho, C. W.; Kim, S. and Yun, Y. S. (2009). *Cinnamon zeylanicum* bark extract and powder mediated green synthesis of nano-crystalline silver particles and its bactericidal activity. Colloids and Surfaces B*: Biointerfaces*, 73(2): 332-338.
52. Ghramh, H. A.; Khan, K. A.; Ibrahim, E. H. and Setzer, W. N. (2019). Synthesis of gold nanoparticles (AuNPs) using *Ricinus communis* leaf ethanol extract, their characterization, and biological applications. *Nanomaterials*, 9: 765, 18 pages.
53. Xu, M.; Liu, J.; Xu, X.; Liu, S.; Peterka, F.; Ren, Y. *et al*. (2018). Synthesis and comparative biological properties of Ag-PEG nanoparticles with tunable morphologies from janus to multicore shell structure. Materials, 11(10): 1787.
54. Faraj, M. M. and AL-Jobor, K. M. (2020). Green synthesis of silver nanoparticles fsing tomato (*Lycopersicon esculentum*) extracts and evaluation of their antifungal activity. Plant Archives,20 (2): 5777-5786.
55. Waris, M.; Nasir, S.; Rasule, A. and Yousaf, I. (2020). Evaluation of larvicidal

efficacy of *Ricinus communis* (Castor) plant extract and synthesized green silver nanoparticles against *Aedes albopictus*. Journal Arthropod-Borne Dis., 14(2): 162–172.

56. Jegadeeswaran, P.; Rajeshwari, S. and Venckatesha. R. (2012). Green synthesis of silver nanoparticles from extract of *padina tetrastromatica* leaf. *Digest Journal of* Nanomaterials and Biostructures. 7, 3. 991-998.
57. Mukherjee, S.; Chowdhury, D.; Kotcherlakota, R. and Patra, S. (2014). Potential theranostics application of bio-synthesized silver nanoparticles (4-in-1 system). Theranostics, 4(3):316.
58. Das, G.; Patra, J. K.; Nagaraj Basavegowda, C. N. V. and Shin, H. S. (2019). Comparative study on antidiabetic, cytotoxicity, antioxidant and antibacterial properties of biosynthesized silver nanoparticles using outer peels of two varieties of *Ipomoea batatas* (L.) Lam. International Journal of Nanomedicine. 14: 4741.
59. Al-Ahmer, S. D., Shami, A. M., & AL-Saadi, B. Q. H. (2018). Using of Hybrid Nanoantibiotics as Promising Antimicrobial Agent. Iraqi Journal of Biotechnology, *17*(3).